

## Comparative Anticancer Activity and Molecular Docking of Different Isatin-Based Scaffolds

BRYAN ALEJANDRO ESPINOSA-RODRIGUEZ, AISSA MICHELLE NIETO-MORENO,  
EDER UBALDO ARREDONDO-ESPINOZA,  
FRANCISCO GUADALUPE AVALOS-ALANÍS and ISAIAS BALDERAS-RENTERIA

*School of Chemistry, Universidad Autonoma de Nuevo Leon (UANL),  
San Nicolás de los Garza, Nuevo Leon, Mexico*

**Abstract.** *Background/Aim: To identify the best of three isatin-based scaffolds in terms of anticancer activity. Materials and Methods: Synthesis of isatin-based scaffolds was performed through a reaction to form Schiff bases. In silico analyses consisted of a target prediction with the Swiss Target Prediction tool and a molecular docking by AutoDock Vina. Anticancer activity and cytotoxicity were determined using the WST1 viability assay. Results: Three scaffolds (IA, IB, and IC) were synthesized and confirmed with good reaction yields. The Swiss Target Prediction tool showed a trend towards kinases. Molecular docking assays demonstrated higher affinity of IC towards CDK2. Anticancer activity assays identified IC as the most active against the cancer cell lines. Cytotoxicity results in non-cancer cells suggested a lack of selectivity. Conclusion: The scaffold IC was identified as the best in terms of anticancer activity and these effects may be due to inhibition of CDK2, as evidenced by molecular docking.*

Cancer is a group of pathologies characterized by uncontrolled proliferation that leads to the formation of tumors with the ability of performing invasion and metastasis. The etiology of cancer is multifactorial and includes both genetic and environmental factors (1). According to data from the Global Cancer Observatory (GLOBOCAN), 19.2 million new cases and almost 10 million deaths from cancer were reported worldwide in 2020. Furthermore, an increase of 47% is expected in the number of new cases by 2040 (2).

Currently, chemotherapy remains the principal therapy of choice in the treatment of most types of cancer (3). However,

*Correspondence to:* Dr. Isaias Balderas Rentería, Professor, School of Chemistry, Universidad Autónoma de Nuevo León, Universidad avenue w/n, Ciudad Universitaria, San Nicolás de los Garza, Nuevo Leon, Mexico. E-mail: isaias.balderasrn@uanl.edu.mx

*Key Words:* Isatin, Schiff bases, molecular docking simulation, neoplasms, cyclin-dependent kinases.

the development of short and long-term side effects, as well as the development of drug resistance by tumors limit its clinical efficacy (4-6). For this reason, the design and development of new anticancer agents have become a priority in medicinal chemistry.

The Hallmarks of Cancer, published by Hanahan and Weinberg in 2000 (7) and 2011 (8), include a set of ten cellular and molecular characteristics that are common in tumors (except for invasion and metastasis only present in malignancies) and important for their establishment, growth, and survival. Since it was published ten years ago, significant discoveries about cancer biology have been made (9). However, the contribution of Hallmarks of Cancer to the development of targeted therapy led to the design of many new approved drugs directed to control one or more of these hallmarks.

Many cell-cycle regulatory proteins and receptor tyrosine kinases have been identified as key players in sustaining proliferative signaling, evading growth suppressors, and modifying other hallmarks. For instance, cyclin-dependent kinases (CDK) are a family of regulatory proteins that control cell cycle progression. In order for CDKs to control the different cell cycle transitions, they must complex with different cyclins that direct kinase activity towards specific substrates. Through phosphorylation reactions, the cyclin-CDK complexes can activate or inhibit essential proteins for cells to advance through the cell cycle, especially towards the S and M phases (10). In some types of cancer, the activity of CDKs is increased, especially that of CDK2 and CDK4/6, leading to greater cell proliferation (10). The CDK4/6 inhibitors palbociclib and ribociclib have been successfully implemented in the treatment of breast cancer (11). However, the development of CDK2 inhibitors has not shown the same progress, despite representing a potential therapeutic target. Similarly, activation of receptor tyrosine kinases due to the active release of growth factors by the tumor stromal cells can lead to sustained proliferation (12). Also, as a consequence of genomic instability, there are gain-

of-function mutations in many receptor tyrosine kinases that lead to activation of receptors more frequently or longer (13). For instance, epithelial growth factor receptor (EGFR) is commonly overexpressed in some types of epithelial cancer, and dependence of tumors on mutated forms of EGFR to survive has been reported (14). Erlotinib and gefitinib are approved drugs that inhibit EGFR by binding to the cytoplasmic kinase domain. Both drugs are competitive inhibitors that block the binding of ATP to the kinase domain of EGFR (14). Since their approval, non-small cell lung cancer has been their primary indication.

Natural products represent an inexhaustible source of new substances with anticancer potential. Indeed, much of the current chemotherapy (> 60%), directly or indirectly, comes from natural products (15). In recent years, indole-derived natural products have gained relevance in medicinal chemistry due to their inhibitory activity on receptor tyrosine kinases (16, 17).

Isatin [1] is an endogenous by-product of the oxidative metabolism of indole (Figure 1). In the past years, isatin and its derivatives have shown antimicrobial, anticancer, and more recently, neuroprotective effects (18, 19). In cancer, isatin and its derivatives appear to inhibit a wide repertoire of molecular targets relevant to cell proliferation and signaling pathways. Some of these targets belong to the cyclin-dependent kinases family and receptor tyrosine kinases.

Isatin is a scaffold that has been included in some experimental drugs (*e.g.*, semaxinib [2]) and in the antiangiogenic drug sunitinib [3] used in the treatment of renal and gastrointestinal tumors (Figure 1). Synthesis of isatin-based scaffolds has focused mainly on the generation of Schiff bases that incorporate different nitrogen-containing heterocycles at positions 1, 3, or both, to generate isatin hydrazones (Figure 1). Sunitinib combines a pyrrolic component with the isatin structure. Some heterocycles that have been used for the synthesis of isatin hydrazones have shown a promising antiproliferative effect in recent years including imidazole (20), phthalazine/quinoxaline/quinoxaline (21), thiazole (22), and triazole (23). In addition to its biological relevance, the formation of Schiff bases allows the easy and quick addition of different structural moieties to isatin, therefore, at the synthetic level, this also represents an advantage.

The design and synthesis of CDK2 inhibitors using isatin-based scaffolds have been previously reported (24-26). However, unlike the vast number of variants mentioned previously, only a few biologically active scaffolds against CDK2 have been identified (5, 6, and 7 in Figure 1). However, a comparison of its anticancer activity, cytotoxicity in non-cancer cells, and its lead likeness are not available. For this reason, this work performed the synthesis, *in vitro* cytotoxicity evaluation, and *in silico* molecular docking of three isatin-based scaffolds, analogous to 5, 6, and 7, with the aim to identify the best scaffold in

terms of biological activity and its potential for the design of new anticancer drugs.

## Materials and Methods

**General information.** All reagents for chemical synthesis were purchased from Sigma-Aldrich (Toluca, Mexico City, MX) unless otherwise specified. The solvents used in the synthesis and purification process were purchased from local commercial distributors. All solvents used in reactions were reagent grade. Distilled industrial grade solvents were used in the purification process. <sup>1</sup>H-NMR and <sup>13</sup>C-NMR spectra were performed on a Bruker instrument at 400 MHz and 100 MHz, respectively, using tetramethylsilane (TMS) as internal standard and DMSO-d<sub>6</sub> as solvent.

### Chemistry

**General procedure for the synthesis of isatin-based scaffolds.** The synthesis of 3-hydrazineylideneindolin-2-one (IA), 4-methyl-N'-(2-oxoindolin-3-ylidene) benzenesulfonohydrazide (IB) and 3,3'-(hydrazine-1,2-diylidene)bis(indolin-2-one) (IC) was carried out through a condensation reaction between isatin and three different raw materials: hydrazine (a), p-toluenesulfonylhydrazide (b) and 3-hydrazineylideneindolin-2-one (c) (Figure 2). The general process began with the dissolution of 500 mg of isatin (1 eq.) in 5 ml of methanol (MeOH) for 5 minutes. Subsequently, 2.5 eq. of raw material a), b) or c) was added. After this, the reaction was refluxed (65°C) until exhaustion of the limiting reagent (isatin). The reaction to form the Schiff bases was based on (27). The progress of the reaction was monitored by thin-layer chromatography (TLC).

After completion of the reaction, according to TLC, the reaction mixture was cooled (4°C) for one hour. After this, the mixture was vacuum filtered and the retained solid was washed using cold methanol (MeOH). The solid obtained was dried in an oven at 65°C. Subsequently, the weight was recorded and recrystallized using ethanol (EtOH). Crystals were vacuum filtered and washed using cold EtOH. Finally, the crystals were dried in an oven at 80°C. The chemical structure of the products was confirmed by <sup>1</sup>H-NMR, <sup>13</sup>C-NMR, and HRMS.

**3-Hydrazineylideneindolin-2-one (IA)** (28). Yellow crystals. <sup>1</sup>H-NMR (400 MHz, DMSO-d<sub>6</sub>) δ 10.69 (s, 1H), 10.54 (d, J=14.5 Hz, 1H), 9.65 (d, J=14.5 Hz, 1H), 7.36 (d, J=7.56 Hz, 1H), 7.15 (td, J=7.68, 1.1 Hz, 1H), 6.97 (td, J=7.56, 0.81 Hz, 1H), 6.86 (d, J=7.68 Hz, 1H); <sup>13</sup>C-NMR (100 MHz, DMSO-d<sub>6</sub>) δ 163 (C=O), 139, 127, 126, 122, 121, 117, 110; HRMS calculated for C<sub>8</sub>H<sub>7</sub>N<sub>3</sub>O: *m/z* 161.0589; found for C<sub>8</sub>H<sub>7</sub>N<sub>3</sub>O: *m/z* 161.0589.

**4-Methyl-N'-(2-oxoindolin-3-ylidene)benzenesulfonohydrazide (IB)**. Yellow crystals. <sup>1</sup>H-NMR (400 MHz, DMSO-d<sub>6</sub>) δ 12.52 (s, 1H), 11.23 (s, 1H), 7.86 (d, J=8.24 Hz, 2H), 7.43 (m, 3H), 7.34 (td, J=7.8, 1.2 Hz, 1H), 7.04 (td, J=7.64, 0.84 Hz, 1H), 6.89 (d, J=7.8 Hz, 1H), 2.36 (s, 3H); <sup>13</sup>C-NMR (100 MHz, DMSO-d<sub>6</sub>) δ 162 (C=O), 145, 142, 137, 135, 132, 130, 128, 123, 121, 119, 111, 21 (CH<sub>3</sub>); HRMS calculated for C<sub>15</sub>H<sub>13</sub>N<sub>3</sub>O<sub>3</sub>S: 315.0678; found for C<sub>15</sub>H<sub>13</sub>N<sub>3</sub>O<sub>3</sub>S: *m/z* 315.0678.

**3,3'-(Hydrazine-1,2-diylidene)bis(indolin-2-one) (IC)** (28). Red powder. <sup>1</sup>H-NMR (400 MHz, DMSO-d<sub>6</sub>) δ 11.02 (s, 2H), 7.52 (d, J=7.48 Hz, 2H), 7.42 (td, J=7.74, 1.18 Hz, 2H), 7.02 (td, J=7.62, 0.66 Hz, 2H), 6.92 (d, J=7.8 Hz, 2H); <sup>13</sup>C-NMR (100 MHz, DMSO-d<sub>6</sub>) δ 163 (C=O), 145.6, 145.2, 134, 128, 123, 116, 111;

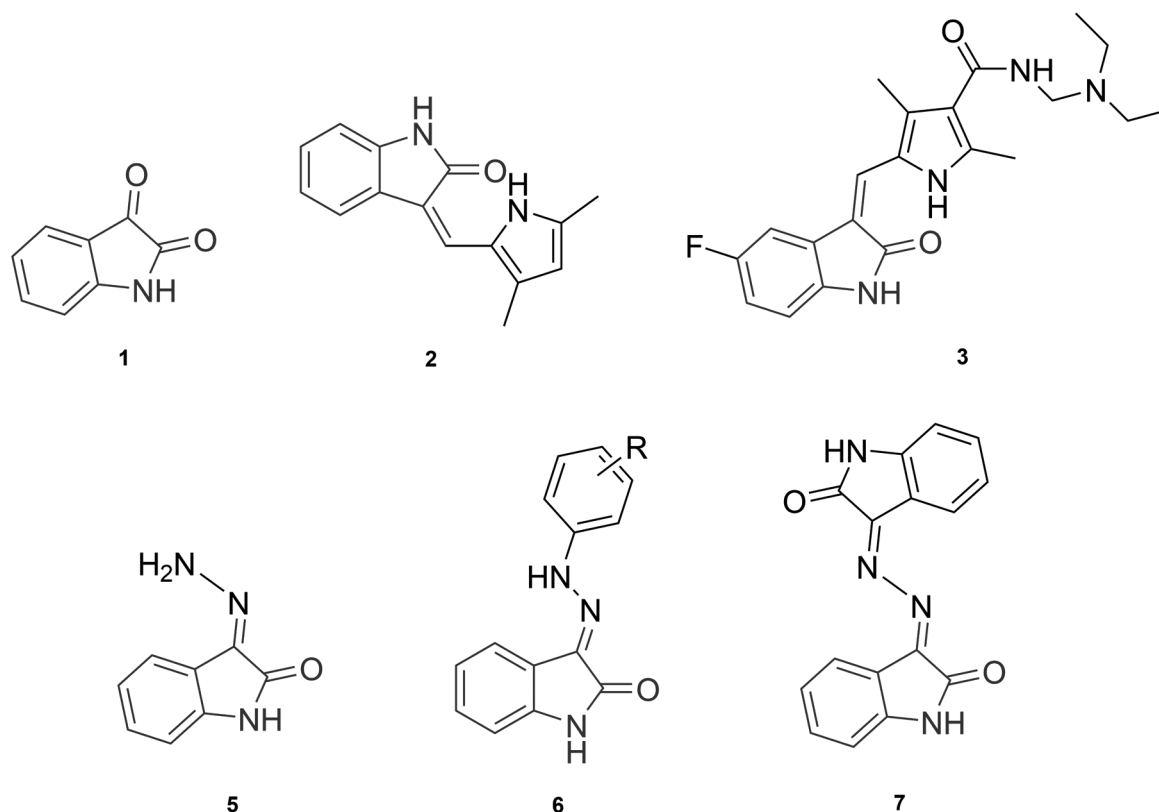


Figure 1. Isatin and different isatin-based scaffolds.

HRMS calculated for  $C_{16}H_{10}N_4O_2$ : 290.0804; found for  $C_{16}H_{10}N_4O_2$ :  $m/z$  290.0804.

**In silico assays.** The three isatin-based scaffolds, IA, IB, and IC, were subjected to target prediction analysis using the SwissTargetPrediction tool from the Swiss Institute of Bioinformatics (29). Those targets predicted for isatin-based scaffolds that belonged to the kinase family were collected. After this, molecular docking was carried out using AutoDock Vina between three molecular targets and the isatin-based scaffolds (30). Molecular dockings were carried out in the rigid modality, and binding energies were recorded. The docking procedure was validated by redocking. Finally, molecular modeling of the resulting docking assays was carried out in University of California San Francisco (UCSF) Chimera (31) with the aim of identifying structural and functional differences in the types and modes of binding of IA, IB, or IC with the molecular targets.

**In vitro anticancer and cytotoxicity assays.** Cytotoxicity of the isatin-based scaffolds was determined using the WST1 viability assay. This assay is based on the metabolic ability of viable cells to reduce the WST1 salt into formazan by mitochondrial dehydrogenases (32). In order to evaluate the cytotoxic effect on cancer cells, the MCF-7 and PC-3 cell lines for breast cancer and prostate cancer, respectively, were used. Finally, cytotoxicity in non-cancer cells was assessed, using the monkey kidney cell line VERO.

The general procedure in every cell line began with the trypsinization of the cells using 0.5 ml of trypsin and incubating them at 37°C for 2 min. Subsequently, 1 ml of medium was added to the cells and the suspension was collected in a 15 ml Falcon tube and centrifuged at  $300 \times g$  for 10 min. The supernatant was discarded, and the pellet was resuspended with 4 ml of medium. Cell counting was carried out using 20  $\mu$ l of this suspension in the Neubauer chamber. An aliquot of this suspension was taken and made to a final volume sufficient to place 5000 cells per well in a 96-well plate. The cells were incubated for 24 h at 37°C in a humidified atmosphere of 5%  $CO_2$ . At the end of the incubation period, 100  $\mu$ l of the compounds were added at the corresponding concentrations. These were evaluated in quadruplicate. In addition, 100  $\mu$ l of negative (medium) and positive (lapatinib) controls were added. The plate with the experimental treatments was incubated for 24 h at 37°C in a humidified atmosphere of 5%  $CO_2$ . Following this, the medium was removed from the 96-well plate, and 100  $\mu$ l of a 5% WST1 solution was added to each well. The 96-well plate with the WST1 was incubated for 2 h at 37°C in a humidified atmosphere of 5%  $CO_2$ . Finally, the optical density was read on an ELISA microplate reader ELx800 (Biotek, Winooski, VT, USA) at 450 nm (33).

The biological evaluation was divided into two stages: 1) exploratory analysis of the three isatin-based scaffolds synthesized at 100  $\mu$ M in the three cell lines mentioned above, and 2) determination of the half-maximal inhibitory concentration ( $IC_{50}$ ) of those compounds that showed cytotoxicity in the exploratory analysis.

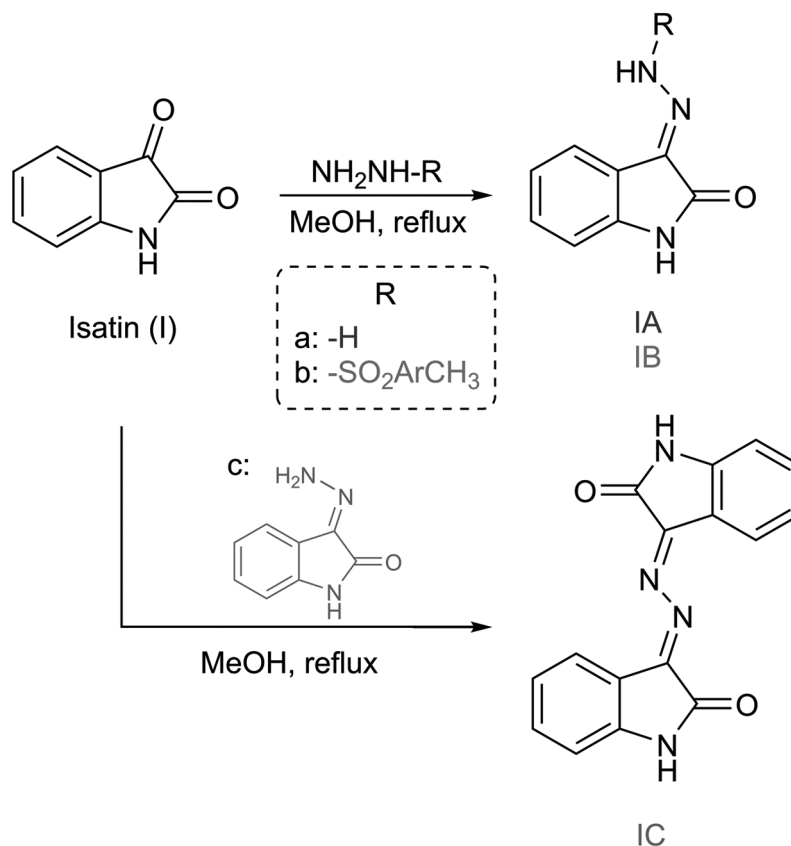


Figure 2. Scheme of synthesis for isatin-based scaffolds. Synthesis of IA or IB (top) consisted of a condensation reaction between isatin and two different reagents, a) hydrazine or b) *p*-toluenesulfonylhydrazide, to produce the corresponding products. Synthesis of IC (bottom) consisted of a condensation reaction between isatin and c) 3-hydrazineylideneindolin-2-one (IA).

**Statistical analysis.** The results of the exploratory analyses were subjected to statistical analysis using the Kruskal–Wallis test. The IC<sub>50</sub> results were subjected to statistical analysis using the *t*-Student test. All the statistical tests were carried out in IBM SPSS statistics (IBM corp. Armonk, NY, USA).

## Results

**Chemistry.** Synthesis of the isatin-based scaffolds began with the optimization of the Schiff base formation reaction. For this step, the generation of the IA was taken as a model reaction to identify the best conditions of synthesis. Initially, the isatin/hydrazine equivalent ratio was modified, altering the reaction yield in consequence. With a 1:1 ratio, a 65% yield was obtained; with a 1:2.5 ratio a yield of 95% was obtained; and with a 1:13 ratio, a yield of 81% was obtained. Furthermore, in the 1:1 ratio, the reaction time was longer (>3 h) compared to the time of the 1:2.5 (30 min) and 1:13 (30 min) ratios. With respect to the purification step, the efficiency of column chromatography was compared against

Table I. Reaction yields obtained for isatin-based scaffolds synthesis.

Isatin-based scaffold	Reaction yield (%)
IA	95
IB	68
IC	95

recrystallization. However, the use of recrystallization was quickly defined as the preferred method for purification due to the intrinsic degradation of the scaffolds caused by the Schiff base hydrolysis reaction induced by the acidic behavior of silica. EtOH was selected as the solvent for recrystallization. After this optimization process, the remaining IB and IC scaffolds were synthesized using the optimized reaction conditions. The reaction yields obtained for the scaffolds using these conditions are shown in Table I. Chemical structures of IA, IB, and IC were confirmed by <sup>1</sup>H-NMR, <sup>13</sup>C-NMR, and HRMS.

Table II. Predicted targets for isatin-based scaffolds employing SwissTargetPrediction.

Isatin-based scaffold	Predicted targets (common names)	Targets selected for docking
IA	MET, CDK2 and CDK1	GSK-3 $\beta$
IB	GSK-3 $\beta$ , JAK3, JAK2, CDK1, CDK2, EGFR, SYK, TGF $\beta$ R1, MAPK8, CHEK1, CDK5R1/CDK5, GSK-3 $\alpha$ , DYRK1A, CDK5, MAPK9, JAK1, TYK2, RAF1, PDPK1, PRKDC, MAPK14, GAK, ATR, AURKA, IGF1R, PRKCA, RET, DBF4/CDC7, PTK2, and ABL1	CDK2 EGFR
IC	MET, PTK2, CDK5R1/CDK5, STK33, JAK1, ATR, GSK-3 $\beta$ , GSK-3 $\alpha$ , PRKDC, ATM, LCK, SYK, CSF1R, JAK3, JAK2, BRAF, FGFR1, and CDK5	

*In silico* assays. The target prediction results in the Swiss Target Prediction tool for the three isatin-based scaffolds showed a trend in their affinity toward kinases, *e.g.*, CDK2, CDK1, and GSK-3 $\beta$ . Based on the predictions of each molecule and the concordance with previous reports, CDK2, GSK-3 $\beta$ , and EGFR were selected, and molecular docking was carried out using AutoDock Vina (Table II).

Molecular docking results showed that IA possessed high binding energies against all the molecular targets tested. The scores went from  $-6.6$  kcal/mol to  $-6.1$  kcal/mol, indicating a low affinity towards them. On the other hand, IB and IC showed low binding energies going from  $-9.5$  kcal/mol to  $-8.2$  kcal/mol. These results indicated the ability to establish moderate or strong interactions with the tested targets (Table III). IB and IC demonstrated a high affinity for CDK2, obtaining the highest binding energies ( $-9.3$  kcal/mol and  $-9.5$  kcal/mol, respectively) of all scaffolds tested.

Molecular modeling of the IB/CDK2 complex demonstrated the establishment of one hydrogen bond and several Van der Waals forces between the scaffold and the different amino acid residues at the ATP-binding site of CDK2. The amino acid residue implicated in the hydrogen bond was His84 (Figure 3). Similarly, IC/CDK2 complex showed the ability of IC to establish Van der Waals forces and two hydrogen bonds involving Leu83 and His84.

*In vitro* anticancer and cytotoxicity assays. Anticancer activity of the three isatin-based scaffolds was assessed by the WST1 cell viability assay, as previously described. MCF-7 and PC-3 cell lines were selected in response to the high incidence of breast and prostate cancer (2). In the exploratory analysis (at  $100 \mu\text{M}$ ), a low cytotoxicity ( $\text{IC}_{50} > 100 \mu\text{M}$ ) for the IA and IB scaffolds was observed in the MCF-7 and PC-3 cell lines. Furthermore, no statistically significant difference was observed between IA and IB compared to isatin ( $p > 0.05$ ). In the case of the IC scaffold, high cytotoxicity was observed in the MCF-7 and PC-3 cell lines with a statistically significant difference compared to the IA and IB scaffolds ( $p < 0.05$ ) (Figure 4). For this reason, we proceeded to

Table III. Binding energies (kcal/mol) for molecular docking among selected kinases and isatin-based scaffolds.

Target	PDB ID	Binding energy (kcal/mol)		
		IA	IB	IC
CDK2/Cyclin A	2I40	$-6.6$	$-9.3$	$-9.5$
EGFR	5U8L	$-6.1$	$-8.5$	$-8.2$
GSK3 $\beta$	6Y9R	$-6.1$	$-8.3$	$-8.9$

determine the  $\text{IC}_{50}$  of IC in these cells, obtaining values of  $19.07 \mu\text{M}$  and  $41.17 \mu\text{M}$  in MCF-7 and PC-3 cells, respectively. In addition, a statistically significant difference was detected between the IC activity compared to the positive control lapatinib whose  $\text{IC}_{50}$  were  $50.61 \mu\text{M}$  and  $32.4 \mu\text{M}$  in MCF-7 and PC-3 cells, respectively ( $p < 0.05$ ) (Table IV).

Cytotoxicity in non-cancer cells of the three scaffolds was evaluated by the same method in the VERO cell line. The results obtained at concentrations of  $100 \mu\text{M}$  showed that the IA and IB scaffolds presented null cytotoxicity towards VERO cells. Furthermore, there was no statistically significant difference between the scaffolds and isatin ( $p > 0.05$ ), but there was compared to the IC platform, which showed high cytotoxicity at concentrations of  $100 \mu\text{M}$  ( $p < 0.05$ ) (Figure 4). For this reason, we proceeded to determine its  $\text{IC}_{50}$  whose value was  $37.78 \mu\text{M}$ , showing a statistically significant difference compared to lapatinib whose  $\text{IC}_{50}$  was greater than  $100 \mu\text{M}$  ( $p < 0.05$ ) (Table IV).

## Discussion

Synthesis of IA and IC has been reported previously (28). At the time of writing this article, there were no reports on the synthesis of IB. However, the synthesis of structurally similar molecules has been reported, although with some differences in functional groups or their structural

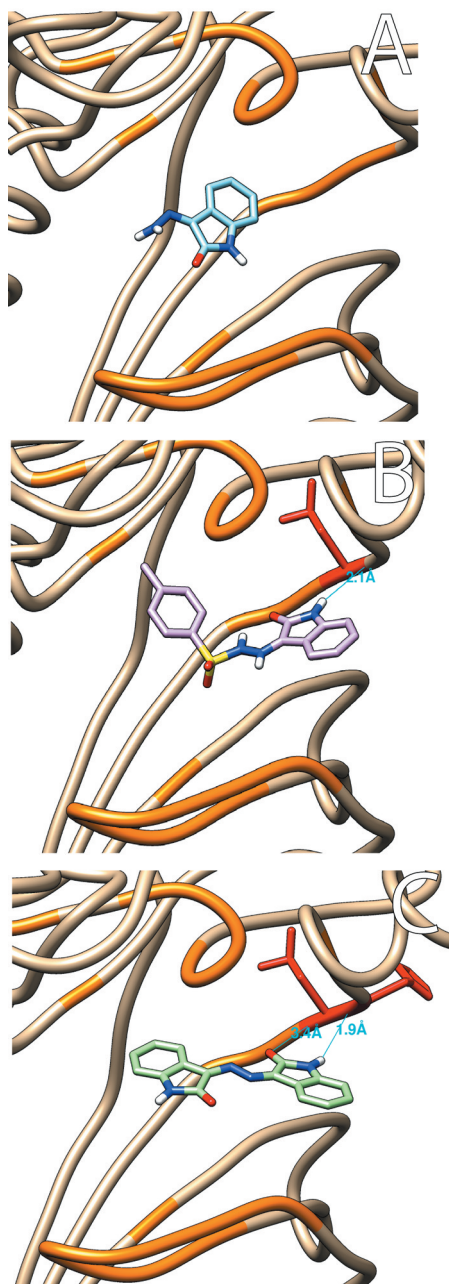


Figure 3. Molecular modelling for IA/CDK2, IB/CDK2 and IC/CDK2 complexes. A. IA showed no establishment of hydrogen bonds in the nucleotide binding site of CDK2. B. IB established a hydrogen bond with His84 in the nucleotide binding site of CDK2. C. IC established two hydrogen bonds with Leu83 and His84 in the nucleotide of CDK2. Nucleotide binding site of CDK2 was highlighted in orange and those amino acid residues involved in hydrogen bonds were highlighted in red.

arrangements. The reaction yield reported by Bramson *et al.* for this type of scaffolds was close to 100% (25); and that reported by Eldehna *et al.* was 65% (34), the latter being the closest to that obtained for the synthesis of IB

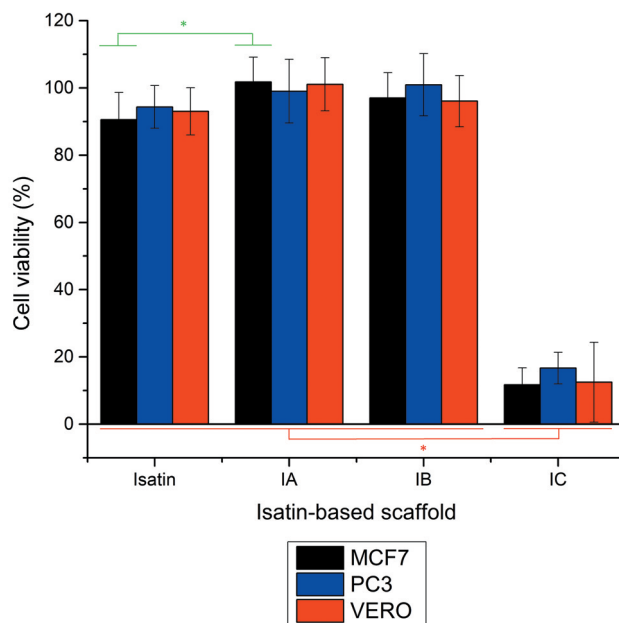


Figure 4. Cell viability of different cell lines treated with isatin-based scaffolds at 100  $\mu\text{M}$ . Cell viability of MCF-7 (black), PC-3 (blue) and VERO (red) cells treated with isatin, or isatin-based scaffolds are shown with its corresponding standard deviation (SD) marks. There was a statistically significant difference on cell viability between isatin and IA in MCF-7 cells (green line). Also, there were statistically significant differences on cell viability between isatin, IA and IB vs. IC in MCF-7, PC-3, and VERO cells (red line). \* $p < 0.05$ .

(68%). In the case of IC, the reaction yields obtained here (95%) were better than those reported by Liang *et al.* in the synthesis of bis-isatin dimers, whose values were between 60-85% (26).

Regarding the *in silico* analyses, the results obtained here for the target prediction agreed with those reported by Bramson *et al.* and Fu *et al.* who synthesized isatin-based scaffolds with affinity for CDK2 and GSK3 $\beta$ , respectively (25, 35). Furthermore, it has been reported that molecules structurally similar to indole, such as isatin, have affinity towards kinases (16, 17, 36). This suggests a possible structural homology of indole scaffolds with adenine from ATP. On the other hand, results derived from molecular docking showed good correlation with interactions of previously reported CDK2 inhibitors. Consistent with our results, the interactions of isatin-based scaffolds analogous to IB with Ile10, Phe85, Asp86, and Leu87 at the ATP-binding site of CDK2 have been previously reported (25). Indirubin derivatives, structurally similar to IC, have shown similar interactions in CDK2 with Ile10, Glu81, and Leu83, leading to inhibition of the enzyme ( $\text{IC}_{50} = 0.01\text{-}4 \mu\text{M}$ ) (37). Furthermore, the interactions were maintained even in the

Table IV. Half-maximal inhibitory concentration for isatin-based scaffolds and lapatinib in MCF-7, PC-3, and VERO cell lines.

Cell line	Compound	IC <sub>50</sub> ± SD
MCF-7	IA	>100 µM
	IB	>100 µM
	IC	19.07±4.02 µM
PC-3	Lapatinib	50.61±12.83 µM
	IA	>100 µM
	IB	>100 µM
	IC	41.17±4.52 µM
VERO	Lapatinib	32.39±2.13 µM
	IA	>100 µM
	IB	>100 µM
	IC	37.78±1.99 µM
	Lapatinib	>100 µM

SD: Standard deviation.

presence of cyclin A complexed with CDK2 (38). These results suggest that IB and IC could be CDK2 inhibitors.

The difference between the binding energies of the IA and IB/IC platforms is in line with that reported by Hu *et al.* (2013) who showed that a simpler molecular scaffold tends to have high molecular promiscuity, while the opposite will occur for a more complex scaffold (39). In this way, the binding energies of the IA scaffold could present an increase due to a lower structural complexity that reduces the possibility of engaging in specific interactions with molecular targets.

*In vitro* anticancer results were consistent with those observed in the molecular docking since a greater anticancer activity of IB and IC scaffolds was expected due to their higher binding energies towards different cell cycle regulatory proteins such as CDK2 and CDK1. However, the results of anticancer activity indicated that only the IC scaffold was biologically active. In agreement with these results, Liang *et al.* reported the *in vitro* anticancer activity of molecules structurally similar to the IC scaffold in the A549, HeLa, HepG2, and SGC-7901 cell lines with values of IC<sub>50</sub> as low as 4.23 µM up to >100 µM (26). The mechanism of action by which the IC scaffold performs its anticancer effect is unknown. However, it has been reported that IC-like molecules down-regulate cyclin B1 and CDK1 (*cdc2*) levels in HepG2 cells (26). The results obtained in the *in silico* analysis demonstrated a high affinity of IC for CDK2, which suggests that a possible mechanism of action for this type of scaffolds could be the inhibition of CDK2 and the subsequent down-regulation of CDK1 and cyclin B1, leading to the arrest of the cell cycle in the G2/M phase, as has been previously reported (26, 40, 41). On the other hand, the IB scaffold lacked *in vitro* biological activity even though molecules with anticancer activity have been reported that operate through the inhibition of CDK1 and CDK2 (25), or

the inhibition of carbonic anhydrase (42). The low cytotoxic activities of the IA and IB scaffolds could be due to the chemical stability that these molecules show towards the cellular hydrolysis of the C=N bond. At the structural level, the IC scaffold presents a conjugated system that gives it a high resistance towards the hydrolysis of the C=N bond, contrary to what was observed in IA and IB. This protection of the conjugated Schiff-bases to the hydrolysis reaction has been reported by Christie *et al.* (43).

Unfortunately, the IC scaffold showed a considerable cytotoxic effect when evaluated in the VERO cell line, indicating a possible lack of selectivity towards cancer cells. Regardless of this, the anticancer activity of IC was comparable to that of lapatinib, a well-known tyrosine kinase inhibitor. Also, it is worth mentioning that here we only evaluated general structures intending to identify the isatin-based scaffold with the best anticancer potential. Furthermore, selectivity could be improved through the addition of new radicals, that operate as guiding groups or generate new non-covalent bonds within the binding site of the protein, to IC as has been described in medicinal chemistry strategies (44). An 8-fold increase in selectivity towards cancer cells has been reported following this approach in isatin derivatives (25).

Targeted drug therapies are changing the way cancer is treated in a positive manner. For instance, imatinib, a BCR-ABL1 inhibitor, has improved the 8-year survival of chronic myeloid leukemia patients in the chronic phase and accelerated phase from 6% and less than 20% to 85% and 75%, respectively (45). Other examples of success are represented by palbociclib and ribociclib, both inhibitors of CDK4/6 have been approved for the treatment of breast cancer. In light of these facts, new research must be performed in discovering or synthesizing new scaffolds directed to relevant targets of cancer. In the past, isatin has been used as a scaffold for the design of anticancer drugs, sunitinib being the most successful case. Despite the relevance of sunitinib, other potential isatin-based drugs are lacking. In the future, more research should be performed on chemical modifications and the biological effects of isatin-based scaffolds. Inhibition of CDK2 should be confirmed through enzymatic assays and other potential biological mechanisms should be explored through transcriptomics, proteomics, or metabolomics assays.

## Conflicts of Interest

The Authors declare no conflicts of interest.

## Authors' Contributions

BAER performed synthesis and biological evaluation, AMNM helped with computational analysis, FGAA supervised the chemical stage of the project, EUAE supervised the biological stage, and IBR designed the original idea and directed the whole project.

## Acknowledgements

The Authors thank UANL for supporting the project FARMC-86133-IBR-18/01. BAER also thanks CONACYT for the graduate scholarship number 932077.

## References

- Balderas-Renteria I, Gonzalez-Barranco P, Garcia A, Banik BK and Rivera G: Anticancer drug design using scaffolds of  $\beta$ -lactams, sulfonamides, quinoline, quinoxaline and natural products. *Drugs advances in clinical trials. Curr Med Chem* 19(26): 4377-4398, 2012. PMID: 22709002. DOI: 10.2174/092986712803251593
- Sung H, Ferlay J, Siegel RL, Laversanne M, Soerjomataram I, Jemal A and Bray F: Global cancer statistics 2020: GLOBOCAN estimates of incidence and mortality worldwide for 36 cancers in 185 countries. *CA Cancer J Clin* 71(3): 209-249, 2021. PMID: 33538338. DOI: 10.3322/caac.21660
- Miller KD, Nogueira L, Mariotto AB, Rowland JH, Yabroff KR, Alfano CM, Jemal A, Kramer JL and Siegel RL: Cancer treatment and survivorship statistics, 2019. *CA Cancer J Clin* 69(5): 363-385, 2019. PMID: 31184787. DOI: 10.3322/caac.21565
- Pearce A, Haas M, Viney R, Pearson SA, Haywood P, Brown C and Ward R: Incidence and severity of self-reported chemotherapy side effects in routine care: A prospective cohort study. *PLoS One* 12(10): e0184360, 2017. PMID: 29016607. DOI: 10.1371/journal.pone.0184360
- Gegechkori N, Haines L and Lin JJ: Long-term and latent side effects of specific cancer types. *Med Clin North Am* 101(6): 1053-1073, 2017. PMID: 28992854. DOI: 10.1016/j.mcna.2017.06.003
- Alfarouk KO, Stock CM, Taylor S, Walsh M, Muddathir AK, Verduzco D, Bashir AH, Mohammed OY, Elhassan GO, Harguindey S, Reshkin SJ, Ibrahim ME and Rauch C: Resistance to cancer chemotherapy: failure in drug response from ADME to P-gp. *Cancer Cell Int* 15: 71, 2015. PMID: 26180516. DOI: 10.1186/s12935-015-0221-1
- Hanahan D and Weinberg RA: The hallmarks of cancer. *Cell* 100(1): 57-70, 2000. PMID: 10647931. DOI: 10.1016/s0092-8674(00)81683-9
- Hanahan D and Weinberg RA: Hallmarks of cancer: the next generation. *Cell* 144(5): 646-674, 2011. PMID: 21376230. DOI: 10.1016/j.cell.2011.02.013
- Fouad YA and Aanei C: Revisiting the hallmarks of cancer. *Am J Cancer Res* 7(5): 1016-1036, 2017. PMID: 28560055.
- Ding L, Cao J, Lin W, Chen H, Xiong X, Ao H, Yu M, Lin J and Cui Q: The roles of cyclin-dependent kinases in cell-cycle progression and therapeutic strategies in human breast cancer. *Int J Mol Sci* 21(6): 1960, 2020. PMID: 32183020. DOI: 10.3390/ijms21061960
- Wu Y, Zhang Y, Pi H and Sheng Y: Current therapeutic progress of CDK4/6 inhibitors in breast cancer. *Cancer Manag Res* 12: 3477-3487, 2020. PMID: 32523378. DOI: 10.2147/CMAR.S250632
- Bussard KM, Mutkus L, Stumpf K, Gomez-Manzano C and Marini FC: Tumor-associated stromal cells as key contributors to the tumor microenvironment. *Breast Cancer Res* 18(1): 84, 2016. PMID: 27515302. DOI: 10.1186/s13058-016-0740-2
- Du Z and Lovly CM: Mechanisms of receptor tyrosine kinase activation in cancer. *Mol Cancer* 17(1): 58, 2018. PMID: 29455648. DOI: 10.1186/s12943-018-0782-4
- Pines G, Köstler WJ and Yarden Y: Oncogenic mutant forms of EGFR: lessons in signal transduction and targets for cancer therapy. *FEBS Lett* 584(12): 2699-2706, 2010. PMID: 20388509. DOI: 10.1016/j.febslet.2010.04.019
- Cragg GM and Newman DJ: Plants as a source of anti-cancer agents. *J Ethnopharmacol* 100(1-2): 72-79, 2005. PMID: 16009521. DOI: 10.1016/j.jep.2005.05.011
- Rathi AK, Syed R, Singh V, Shin HS and Patel RV: Kinase inhibitor indole derivatives as anticancer agents: a patent review. *Recent Pat Anticancer Drug Discov* 12(1): 55-72, 2017. PMID: 27697069. DOI: 10.2174/1574892811666161003112119
- Dhuguru J and Skouta R: Role of indole scaffolds as pharmacophores in the development of anti-lung cancer agents. *Molecules* 25(7): 1615, 2020. PMID: 32244744. DOI: 10.3390/molecules25071615
- Guo H: Isatin derivatives and their anti-bacterial activities. *Eur J Med Chem* 164: 678-688, 2019. PMID: 30654239. DOI: 10.1016/j.ejmech.2018.12.017
- Medvedev A, Kopylov A, Buneeva O, Kurbatov L, Tikhonova O, Ivanov A and Zgoda V: A neuroprotective dose of isatin causes multilevel changes involving the brain proteome: prospects for further research. *Int J Mol Sci* 21(11): 4187, 2020. PMID: 32545384. DOI: 10.3390/ijms21114187
- Taher AT, Khalil NA and Ahmed EM: Synthesis of novel isatin-thiazoline and isatin-benzimidazole conjugates as anti-breast cancer agents. *Arch Pharm Res* 34(10): 1615-1621, 2011. PMID: 22076761. DOI: 10.1007/s12272-011-1005-3
- Abdel-Aziz HA, Eldehna WM, Keeton AB, Piazza GA, Kadi AA, Attwa MW, Abdelhameed AS and Attia MI: Isatin-benzoazine molecular hybrids as potential antiproliferative agents: synthesis and *in vitro* pharmacological profiling. *Drug Des Devel Ther* 11: 2333-2346, 2017. PMID: 28848327. DOI: 10.2147/DDDT.S140164
- Eldehna WM, Al-Wabli RI, Almutairi MS, Keeton AB, Piazza GA, Abdel-Aziz HA and Attia MI: Synthesis and biological evaluation of certain hydrazonoindolin-2-one derivatives as new potent anti-proliferative agents. *J Enzyme Inhib Med Chem* 33(1): 867-878, 2018. PMID: 29707975. DOI: 10.1080/14756366.2018.1462802
- Aneja B, Khan NS, Khan P, Queen A, Hussain A, Rehman MT, Alajmi MF, El-Seedi HR, Ali S, Hassan MI and Abid M: Design and development of Isatin-triazole hydrazones as potential inhibitors of microtubule affinity-regulating kinase 4 for the therapeutic management of cell proliferation and metastasis. *Eur J Med Chem* 163: 840-852, 2019. PMID: 30579124. DOI: 10.1016/j.ejmech.2018.12.026
- Al-Salem HS, Arifuzzaman M, Alkhtani HM, Abdalla AN, Issa IS, Alqathama A, Albalawi FS and Rahman AFMM: A series of isatin-hydrazones with cytotoxic activity and CDK2 kinase inhibitory activity: a potential type II ATP competitive inhibitor. *Molecules* 25(19): 4400, 2020. PMID: 32992673. DOI: 10.3390/molecules25194400
- Bramson HN, Corona J, Davis ST, Dickerson SH, Edelstein M, Frye SV, Gampe RT Jr, Harris PA, Hassell A, Holmes WD, Hunter RN, Lackey KE, Lovejoy B, Luzzio MJ, Montana V, Rocque WJ, Rusnak D, Shewchuk L, Veal JM, Walker DH and Kuypers LF: Oxindole-based inhibitors of cyclin-dependent kinase 2 (CDK2): design, synthesis, enzymatic activities, and X-ray crystallographic analysis. *J Med Chem* 44(25): 4339-4358, 2001. PMID: 11728181. DOI: 10.1021/jm010117d

- 26 Liang C, Xia J, Lei D, Li X, Yao Q and Gao J: Synthesis, *in vitro* and *in vivo* antitumor activity of symmetrical bis-Schiff base derivatives of isatin. *Eur J Med Chem* 74: 742-750, 2014. PMID: 24176732. DOI: 10.1016/j.ejmech.2013.04.040
- 27 Sridhar SK and Ramesh A: Synthesis and pharmacological activities of hydrazones, Schiff and Mannich bases of isatin derivatives. *Biol Pharm Bull* 24(10): 1149-1152, 2001. PMID: 11642321. DOI: 10.1248/bpb.24.1149
- 28 Hassan TAFM, Kadi AA and Abdel-Aziz HAK: Novel N,N'-hydrazino-bis-isatin derivatives with selective activity against multidrug-resistant cancer cells. Washington, U.S. Patent and Trademark Office, 2013. Available at <https://patentimages.storage.googleapis.com/70/7f/8b/ade5ddc4ee005f/US20120252860A1.pdf> [Last accessed on 19th June 2021]
- 29 Daina A, Michielin O and Zoete V: SwissTargetPrediction: updated data and new features for efficient prediction of protein targets of small molecules. *Nucleic Acids Res* 47(W1): W357-W364, 2019. PMID: 31106366. DOI: 10.1093/nar/gkz382
- 30 Trott O and Olson AJ: AutoDock Vina: improving the speed and accuracy of docking with a new scoring function, efficient optimization, and multithreading. *J Comput Chem* 31(2): 455-461, 2010. PMID: 19499576. DOI: 10.1002/jcc.21334
- 31 Pettersen EF, Goddard TD, Huang CC, Couch GS, Greenblatt DM, Meng EC and Ferrin TE: UCSF Chimera – a visualization system for exploratory research and analysis. *J Comput Chem* 25(13): 1605-1612, 2004. PMID: 15264254. DOI: 10.1002/jcc.20084
- 32 Riss TL, Moravec RA, Niles AL, Duellman S, Benink HA, Worzella TJ and Minor L: Cell viability assays. In: *Assay Guidance Manual*. Markossian S, Grossman A, Brimacombe K (eds.). Bethesda (MD): Eli Lilly & Company and the National Center for Advancing Translational Sciences, pp. 359-384, 2004.
- 33 Aguirre-Rentería SA, Carrizales-Castillo JJJ, Del Rayo Camacho Corona M, Hernández-Fernández E, Garza-González E, Rivas-Galindo VM, Arredondo-Espinoza E and Avalos-Alanís FG: Synthesis and *in vitro* evaluation of antimycobacterial and cytotoxic activity of new  $\alpha,\beta$ -unsaturated amide, oxazoline and oxazole derivatives from L-serine. *Bioorg Med Chem Lett* 30(9): 127074, 2020. PMID: 32151467. DOI: 10.1016/j.bmcl.2020.127074
- 34 Eldehna WM, Al-Ansary GH, Bua S, Nocentini A, Gratteri P, Altoukhy A, Ghabbour H, Ahmed HY and Supuran CT: Novel indolin-2-one-based sulfonamides as carbonic anhydrase inhibitors: Synthesis, *in vitro* biological evaluation against carbonic anhydrases isoforms I, II, IV and VII and molecular docking studies. *Eur J Med Chem* 127: 521-530, 2017. PMID: 28109946. DOI: 10.1016/j.ejmech.2017.01.017
- 35 Fu G, Sivaprakasam P, Dale OR, Manly SP, Cutler SJ and Doerksen RJ: Pharmacophore modeling, ensemble docking, virtual screening, and biological evaluation on glycogen synthase kinase-3 $\beta$ . *Mol Inform* 33(9): 610-626, 2014. PMID: 27486080. DOI: 10.1002/minf.201400044
- 36 Prakash CR and Raja S: Indolinones as promising scaffold as kinase inhibitors: a review. *Mini Rev Med Chem* 12(2): 98-119, 2012. PMID: 22372601. DOI: 10.2174/138955712798995039
- 37 Jautelat R, Brumby T, Schäfer M, Briem H, Eisenbrand G, Schwahn S, Krüger M, Lücking U, Prien O and Siemeister G: From the insoluble dye indirubin towards highly active, soluble CDK2-inhibitors. *Chembiochem* 6(3): 531-540, 2005. PMID: 15742375. DOI: 10.1002/cbic.200400108
- 38 Davies TG, Tunnah P, Meijer L, Marko D, Eisenbrand G, Endicott JA and Noble ME: Inhibitor binding to active and inactive CDK2: the crystal structure of CDK2-cyclin A/indirubin-5-sulphonate. *Structure* 9(5): 389-397, 2001. PMID: 11377199. DOI: 10.1016/s0969-2126(01)00598-6
- 39 Hu Y and Bajorath J: Compound promiscuity: what can we learn from current data? *Drug Discov Today* 18(13-14): 644-650, 2013. PMID: 23524195. DOI: 10.1016/j.drudis.2013.03.002
- 40 Mitra J and Enders GH: Cyclin A/Cdk2 complexes regulate activation of Cdk1 and Cdc25 phosphatases in human cells. *Oncogene* 23(19): 3361-3367, 2004. PMID: 14767478. DOI: 10.1038/sj.onc.1207446
- 41 De Boer L, Oakes V, Beamish H, Giles N, Stevens F, Somodevilla-Torres M, Desouza C and Gabrielli B: Cyclin A/cdk2 coordinates centrosomal and nuclear mitotic events. *Oncogene* 27(31): 4261-4268, 2008. PMID: 18372919. DOI: 10.1038/onc.2008.74
- 42 Eldehna WM, Nocentini A, Al-Rashood ST, Hassan GS, Alkahtani HM, Almehezia AA, Reda AM, Abdel-Aziz HA and Supuran CT: Tumor-associated carbonic anhydrase isoform IX and XII inhibitory properties of certain isatin-bearing sulfonamides endowed with *in vitro* antitumor activity towards colon cancer. *Bioorg Chem* 81: 425-432, 2018. PMID: 30219719. DOI: 10.1016/j.bioorg.2018.09.007
- 43 Christie RJ, Anderson DJ and Grainger DW: Comparison of hydrazone heterobifunctional cross-linking agents for reversible conjugation of thiol-containing chemistry. *Bioconjug Chem* 21(10): 1779-1787, 2010. PMID: 20695431. DOI: 10.1021/bc100049c
- 44 Huggins DJ, Sherman W and Tidor B: Rational approaches to improving selectivity in drug design. *J Med Chem* 55(4): 1424-1444, 2012. PMID: 22239221. DOI: 10.1021/jm2010332
- 45 Kantarjian H, O'Brien S, Jabbour E, Garcia-Manero G, Quintas-Cardama A, Shan J, Rios MB, Ravandi F, Faderl S, Kadia T, Borthakur G, Huang X, Champlin R, Talpaz M and Cortes J: Improved survival in chronic myeloid leukemia since the introduction of imatinib therapy: a single-institution historical experience. *Blood* 119(9): 1981-1987, 2012. PMID: 22228624. DOI: 10.1182/blood-2011-08-358135

Received July 21, 2021

Revised August 27, 2021

Accepted August 30, 2021